Chapter 4: APPLICATION OF THE MODEL

The geophysical period 1992-1996 has been very interesting from the point of view of tsunami studies. Eight large earthquakes have generated tsunamis with runup heights exceeding 5*m*. All these events were investigated by an ad-hoc group of primarily Japanese and American scientists referred to as the International Tsunami Survey Team. These surveys were the first since 1983 and they produced high-quality inundation data at exactly the time when inundation codes had started breaking the computational barriers of the shoreline calculations. The watershed event was the Nicaraguan tsunami of September 1, 1992; the initial numerical computations demonstrated the inability of the then-available codes to model even to first-order the inundation patterns. The discrepancies fueled speculations whether it was the seismological models which predicted incorrect initial conditions or whether it was the hydrodynamic models which did not simulate properly the propagation and runup. Subsequent events confirmed that discrepancies existed, but refinements in the hydrodynamic codes have reduced them substantially, focusing the efforts for better predictions to the initial conditions and to the bathymetry and topography resolution. In this section, the predictions of the model presented earlier will be compared with some of the field results, at least those cases when bathymetric and topographic data of sufficient resolution exist to make the comparisons meaningful.

4.1 The tsunami generation model

Development of the models of tsunami generation by an earthquake source is closely related to the studies of the earthquake source mechanism which is a very active topic of seismological research. This aspect of the tsunami wave studies is out of the scope of the dissertation. Nevertheless, since the tsunami source model provides initial conditions for the numerical experiments, this section describes and briefly discuss the model of tsunami source which is used here.

When the earthquake's source is located under the sea bed, part of the earthquake's energy is transmitted into the water body. If the amount of this energy is big enough, the earthquake can generate long gravity waves on the surface of the water, i.e. tsunami waves. Studies show that the portion of the energy transmitted to the tsunami wave generation is not more then 10% of the total energy released by the earthquake (Iida, 1956, Gusyakov, 1976, 1988). The amount of this part of the earthquake energy highly depends on the earthquake source mechanism; for typical tsunamigenic earthquakes only about 1% of the total released energy is contributed to the tsunami wave generation, which implies that only strong earthquakes with M_w greater than 6.8-7.0 can generate a considerable tsunami.

The model of the tsunami generation process used in the dissertation is based on the elastic model of the earthquake source (Gusyakov, 1972). The model assumes compressibility of a liquid layer i.e. of a model of the ocean and elasticity of the underlying halfspace, i.e. of a model of the Earth crust. The displacement-equations of motion of the theory of elasticity for this model are written as follows
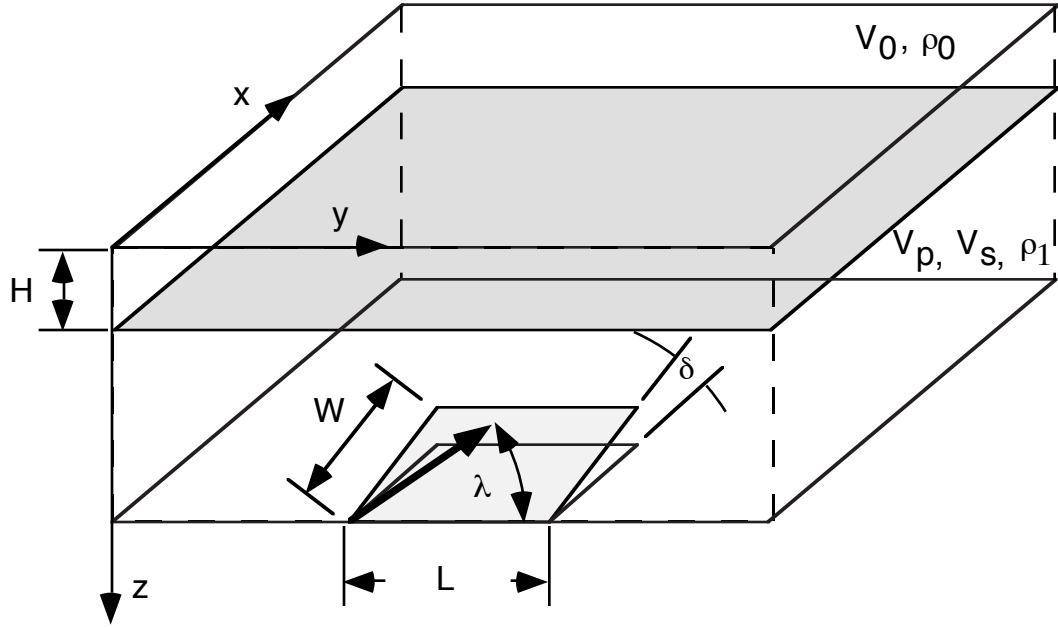
Figure 4.30 Definition sketch of the submarine earthquake source model.

$$V_0 \nabla(\nabla \bullet \mathbf{u}) - g \nabla \bullet (\mathbf{u} \cdot \mathbf{k}) = \frac{\partial^2 u}{\partial t^2}, \quad 0 < z \leq H, \tag{4.37}$$

$$(V_p^2 - V_s^2)\nabla(\nabla \bullet \mathbf{u}) + V_s^2 \nabla^2 \mathbf{u} - g\nabla \bullet (\mathbf{u} \cdot \mathbf{k}) = \frac{\partial^2 u}{\partial t^2}, \quad z > H, \tag{4.38}$$

with boundary conditions on the free surface, $z = 0$

$$V_0^2 \nabla \bullet \mathbf{u} - g u_z \Big|_{z=0} = 0, \tag{4.39}$$

and on the sea floor, $z = H$

$$u_z \Big|_{z=H+0} = u_z \Big|_{z=H-0}, \tag{4.40}$$

78

$$\left.\left(\frac{\partial u_x}{\partial z} + \frac{\partial u_z}{\partial x}\right)\right|_{z=H+0} = 0, \quad \left.\left(\frac{\partial u_y}{\partial z} + \frac{\partial u_z}{\partial y}\right)\right|_{z=H+0} = 0, \tag{4.41}$$

$$\left.\rho_1\left((V_p^2 - V_s^2)\nabla\bullet\mathbf{u} + 2V_s^2\frac{\partial u_z}{\partial z}\right)\right|_{z=H+0} = \left.\rho_0(V_0^2\nabla\bullet\mathbf{u} - gu_z)\right|_{z=H-0}, \tag{4.42}$$

where **u** is displacement, V_0 is speed of sound in the water, $V_{p,s}$ are P and S wave velocities, H is ocean depth, **k** is a unit vector along z, ρ_0 and ρ_1 are density of the water and of the earth crust.

The coupling between the two media is provided by the existence of the gravity field which is taken into account as additional gravity terms in the equation of motion (4.37), (4.38) and in the boundary conditions at the free surface and at the inner interface (4.39) - (4.42).

Poddyapolsky (1968) was the first who used the elastic model to the tsunami generation problem. Assuming compressible fluid, he was able to come up with approximate solutions for the displacement in the far field using the point-source model. Later a similar approach was developed by Alekseev and Gusiakov (1972), Sato and Yamashita (1974), Ward (1980). These authors investigated the conditions of tsunami generation depending on basic source parameters such as depth, source mechanism, rupture velocity, duration of the displacement. The very general conclusions based on this theory are that large tsunami waves are produced by the earthquakes with a shallow source of thrust-type mechanism with a low-angle fault plane and that the duration of the source motion does not affect the tsunami wave very much if less than several minutes. The latter implies that tsunami source

can be considered as an instantaneous movement of the sea-floor for most cases without inducing a substantial error into the tsunami evolution model.

One of the basic limitation of the elastic model is the even bottom of the ocean, because the solution of the fully coupled system with the variable interface between the layers is too complicated problem. On the other hand, the depth of the ocean is a major factor in the tsunami wave propagation. To overcome this problem the following approach is used. The elastic model of tsunami wave is used only as the first step in tsunami wave modeling. It gives either the initial water-wave field displacement, or the deformation of the bottom surface due to the earthquake source. Since the duration of the source movement is very short if compared with the periods of the long gravity water waves, the ground motion during an earthquake does not affect the evolution of the tsunami wave much. Then, the simulation of tsunami wave evolution can be modeled separately from the seismic processes. Thus, the simulation of the tsunami wave is split on two parts:

1. calculation of static bottom displacement for the elastic halfspace with an inner seismic source
2. calculation of the tsunami wave propagation over the incompressible inviscid ocean using some hydrodynamic model.

The results of the first-part modeling are used as initial conditions for the hydrodynamic modeling. The static bottom displacement is usually calculated using the elastic model without consideration of the ocean layer. This approach has become a standard technique since Mansinha, L. and D.E.Smylie (1971) published the formula for the surface deformation calculation. Here, the same principal of the tsunami source model is used. The formula

of static sea-floor deformation developed by Gusyakov (1972) is utilized to calculate the initial conditions for the tsunami propagation and inundation model.

A double-couple-model earthquake source is defined by seven parameters (Figure 4.30), the length of the rupture plane L, the width of the plane W, the depth of the source h, dip angle δ, slip angle λ, strike angle θ and the average slip amount u_0. The moment magnitude of this model source is determined from the formula

$$M_0 = \mu u_0 LW, \tag{4.43}$$

where μ is the rigidity of the earth crust, with a value ranging from 1 to 6×10^{10} N/m^2 depending on the local geological structure.

Table 2 SOURCE PARAMETERS USED FOR SIMULATIONS

Event	L (km)	W (km)	Strike	Dip	Slip	U_0 (m)	M_0 (Nm)	Rigidity (N/m^2)
Kurils	120	100	151°	51°	11°	10	3.6×10^{21}	3×10^{10}
Nikaragua	200	100	302°	16°	187°	3.75	2.2×10^{21}	3×10^{10}
Peru	120	60	340°	15°	96°	4	5.6×10^{20}	2×10^{10}
Okushiri (North) (Central) (South)	90 30 24.5	25 25 25	188 175 163	35 60 60	80 105 105	5.71 2.50 12.0	6.62×10^{21}	3×10^{10}
Mexico (South) (North)	70 100	45 50	296 322	16 16	90 90	2 3	8.5×10^{20}	3×10^{10}

The moment magnitude of the earthquake source as well as depth, dip angle, slip angle and strike angle can be estimated from the seismic waves analysis. In most of the modeled cases the analysis of the seismograms performed by Harvard group is used for the source param-

eters estimation. The so-called Harvard Central Moment Tensor (CMT) solution is available shortly after major earthquakes via Internet and is usually published later (see Dziewonski, et al., 1993a,b,1994a,b). Formula (4.43) is than used to determine the L, W and u_0 of the tsunami source.

In the following sections VTCS-3 will be used to model certain recent tsunami events for which both sufficient resolution bathymetry data and source solution exist. The parameters of the earthquake sources for these events are summarized in Table 2.The simulations will be presented in order of complexity of model applications. The first simulation (the Kuril tsunami) does not use moving boundary conditions. The wall-type totally reflective conditions are assumed for all land boundaries in the computation. The Nicaragua and Peru models use a two-step computational method, this involves a 2+1 simulation without runup, similar to the Kuril case, and then 1+1 runup computations for selected locations. The Hokkaido-Nansei-Oki and Mexico tsunamis are modeled using the 2+1 runup model with the inundation computations applied to all land boundaries.

4.2 The October 4, 1994 South Kuril Islands Earthquake

4.2.1 Introduction

On October 4, 1994, at 1:23 p.m. GMT, an earthquake of magnitude $M_w = 8.2$ (HRV), 8.3 (USGS) struck the southern region of Kuril Islands. Since this area is poorly covered by the regional seismic networks, there is quite large discrepancies in epicenter location estimation by different agencies; different main shock locations are shown in Figure 4.31.
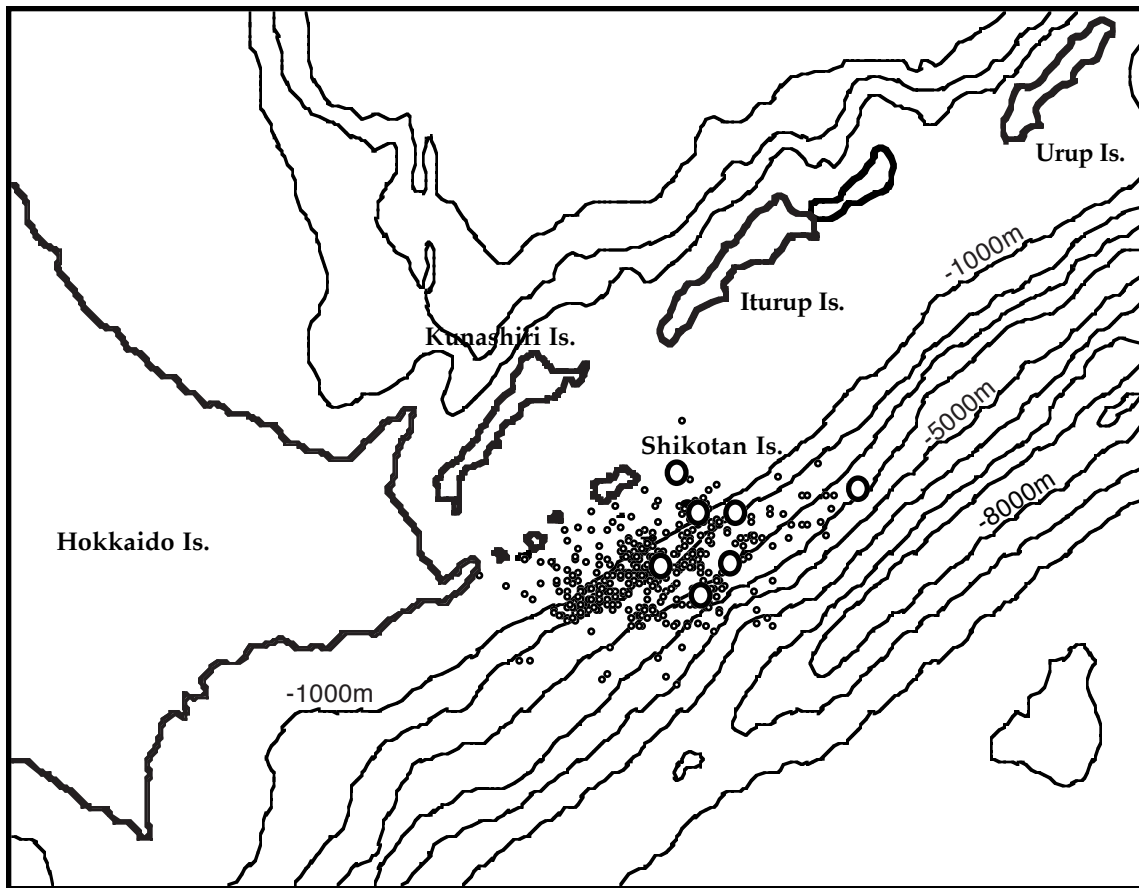
Figure 4.31 One-week-aftershock distribution (small circles) and different estimations of the main shock location (large circles).

On Shikotan Island, one of the South Kuril Islands, located closest to the earthquake epicenter, the ground shaking was extremely intense: the intensity was reported to be between 9 and 10 on the abridged Modified Mercalli Intensity Scale (12 full shake scale). Approximately 1.8m tsunami runup was reported immediately in Nemuro, Japan, and Pacific-wide tsunami warnings were issued, including in the coastal regions of Hawaii, the west coast of the United States and Canada. There were no casualties due directly to the tsunami in spite of its significant runup (approximately 10m high runup was measured in Shikotan Island)

because the coastlines closest to the epicenter were uninhabited. Also, the South Kuril areas have experienced many large earthquake and tsunamis in the past, hence the local people were prepared well for such natural disasters.

4.2.2 The post-tsunami field survey

The tsunami reconnaissance survey was conducted from October 16 through 30, 1994, by fifteen Russian scientists and two members from the United States. Results of the survey and geophysical aspects of this earthquake are reported in Yeh et al. (1995). Tsunami runup height measurements were made in Shikotan, Iturup, Kunashir, and small islands between Shikotan and Hokkaido (e.g. Polonsky, Zeleny, and Yury Islands). Measurements along the Hokkaido coast were carried out by the Tohoku University group in Japan. The measured data were corrected to values of the vertical runup heights from sea level at the time of the tsunami attack.

In Shikotan Island, measurements were made at 85 different locations around the island. Large part of the island's coastline is a series of nearly vertical cliffs which are not readily accessible. All measurements were taken inside bays around the island with flat-sloped beaches which were approachable and had clear runup marks. The measurements were made based on very conservative and strict tsunami runup marks, i.e. only marine-origin objects were considered to be appropriate for tsunami runup marks. The measured runup heights around the island were plotted in Figure 4.32. The values presented in the figure are not individual measurements but the maximum values over all measurements for each particular bay.
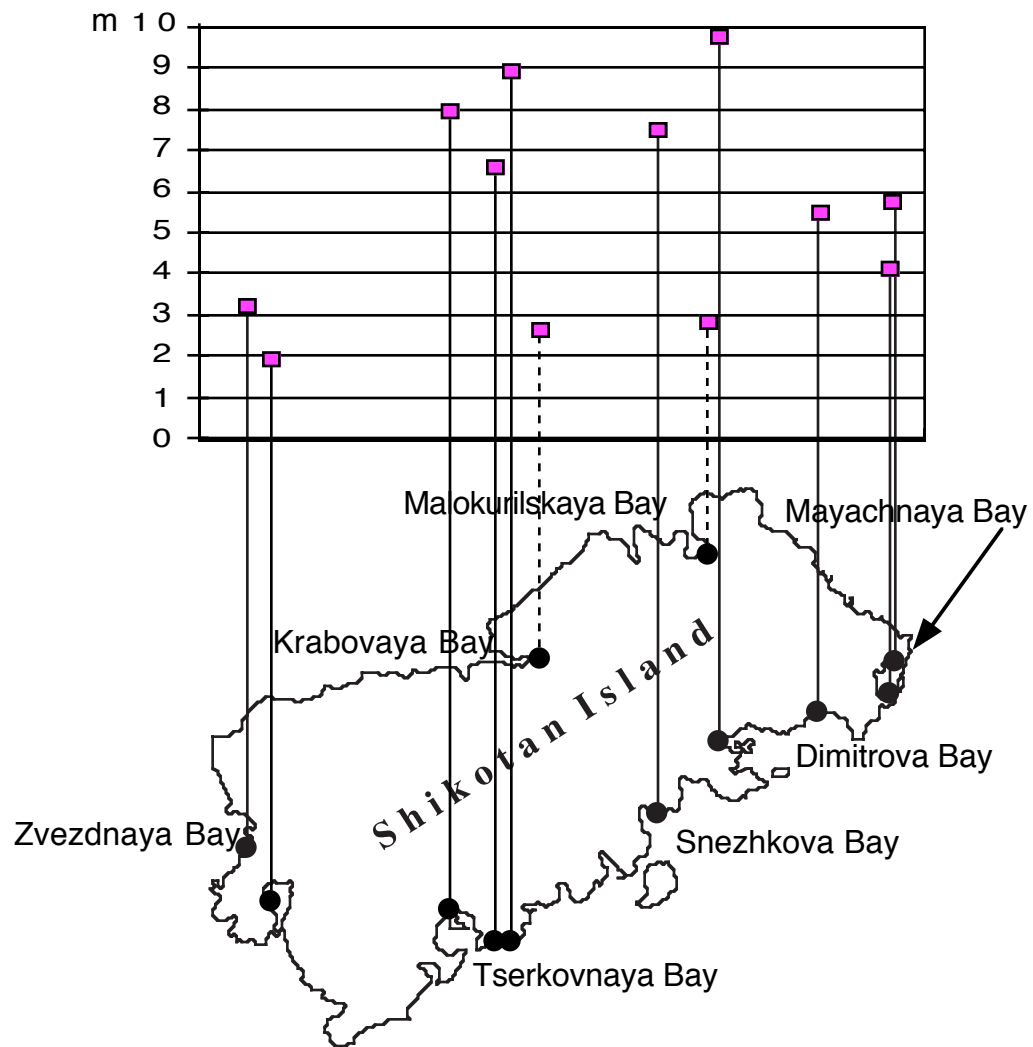
Figure 4.32 Runup measurements around the Shikotan island.

Figure 4.32 shows that the magnitudes of runup are fairly uniform: the average run-up height is $6.07m$ on the south side of the island with a standard deviation of $1.78m$, while on the north side of the island, the average runup height is $2.50m$ with a standard deviation of $0.24m$. The uniformity of the runup distribution along the north coasts facing the tsunami source suggests that the tsunami wave was long enough for the wave not to be affected by

the local features of the coastline. Long penetration distances of the tsunami in spite of the dense vegetation also support the hypothesis of fairly large wavelength of the climbing tsunami, since a longer wave with larger period would have more time to flood all areas bellow the maximum wave height regardless of the local topography or resistance of dense vegetation. An eyewitness report in Malokurilskaya Bay indicated that the leading wave was a leading elevation wave followed by approximately 2.5m of negative wave. The resulting current was so swift that no ship could across the bay entrance nor approach the shore for the first two and a half hours, while the current speed of approximately 6m/sec was reported by an eyewitness. The bottom sounding showed that the water depth at the center of the bay changed from 5m to 8m, evidently due to tsunami scouring effects.

4.2.3 Numerical model

The numerical simulation of this event was carried out using the VTCS-3 code but without the inundation computations. The reason for not including the runup into the computations is twofold. First, the topographical information of the modeled areas was not available at the time of the modeling. Second, as was mentioned in section , the wavelength of the Kuril tsunami was anticipated to be fairly long, which makes the wave less sensitive to the local topographic features. Hence, the calculations without runup modeling may provide acceptable accuracy at least as far as the wave-height distribution pattern is concerned. The TOPO5 bathymetric data was used to generate the computational grid for the modeled area.

The mechanism of the earthquake source was complex and not fully understood at this point, it appears that this is not a typical interplate subduction earthquake but, instead,

the plate buckled perpendicular to the subduction line. Consequently, it is difficult to determine an accurate estimate of the initial sea-bottom deformation. The Harvard University's centroid moment tensor determination for the 1994 Shikotan earthquake was obtained about 6 hours after the main shock. The best double-couple solution consists of two planes, none of which can be considered to represent the low-angle thrust typical for the subduction region interplate event. The first plane dipping under the angle 50° to the S-W strikes almost perpendicular to the trench axis. The second plane with strike direction 52° roughly corresponding bottom lineaments dips under the angle 77° to S-E so that its predominant source mechanism should be the inverse dip-slip fault with considerable (slip angle 128°) strike component. Both models were examined as initial conditions for the tsunami computations. The first fault model was chosen as a primary tsunami source mechanism, since this mechanism is resembling the intra-slab event when the rupture plane tears the subducting oceanic lithosphere with a direction normal to the trench. Tanioka et al. (1995) derived similar conclusions from the joint inversion of geodetic and tsunami data and constructed the source very similar to the one used here. The contours of the associated sea-floor displacement are shown on Figure 4.33. The model source parameters are, area $L \times W = 120 \times 100 km$, Strike = 152°, Dip = 51°, Slip = 11°, $U_0 = 10m$. The moment magnitude of the source is $M_0 = 3.6 \times 10^{21}$ Nm, assuming the rigidity $\mu = 3 \times 10^{11}$ N/m^2.

The results of the computation are compared with the measurements on Figure 4.33. The figure shows that—as was suggested earlier in this section—the model was able to reproduce to first order the pattern of the runup distribution along the coasts close to the tsunami source, even though the inundation computation was not included. Given the qualita-

tive agreement between the field runup data and the threshold model computations, it is clear that the wave height did not change significantly from the 5m depth to the shoreline, suggestive of slow flooding. The evidences collected during the post-tsunami field survey also support the slow-flooding hypothesis for this tsunami (see section).
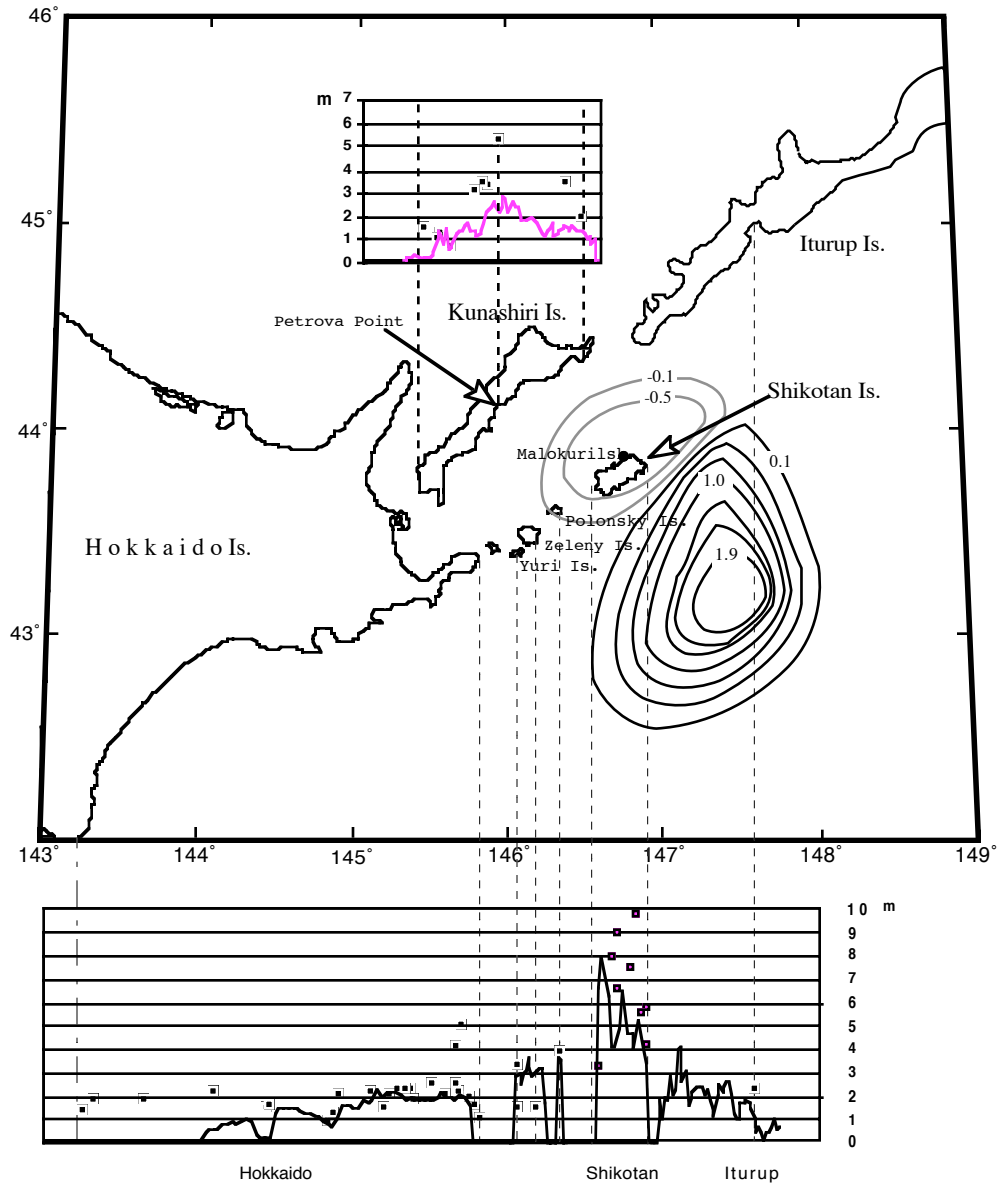

Figure 4.33 Results of the computer simulation of the Kuril tsunami. Contours of the initial sea-floor displacement used as initial conditions are shown on the map. Computed wave heights (solid lines) compared with the highest runup measurements (dots) at each location.